THE ARCHIVE OF MECHANICAL ENGINEERING

VOL. LVIII 2011 Number 1

10.2478/v10180-011-0002-x

Key words: electrostatic precipitation, rigid finite element method, hybrid method, vibration analysis

IWONA ADAMIEC-WÓJCIK *

MODELLING OF SYSTEMS OF COLLECTING ELECTRODES OF ELECTROSTATIC PRECIPITATORS BY MEANS OF THE RIGID FINITE ELEMENT METHOD

The paper presents a model of a rapping system of an electrostatic precipitator. The rapping system consists of a set of collecting electrodes hanging on a suspension bar and braced together in a brushing bar. The suspension and brushing bars are modeled using the rigid finite element method, while the collecting plates are modeled using the hybrid method. The method combines the rigid finite element method with the classical finite element method. As a result, the mass matrix is diagonal. Some results of numerical simulations concerning free vibrations of the collecting plates and the influence of the number of elements, into which the plate is divided, on the vibrations of the rapping system are presented.

1. Introduction

An increasing world-wide interest in ecological issues, such as global warming, air quality and acid rain, results in an obligation to reduce pollution from industrial processes. One of the most common industrial appliances used to control air pollution in power plants are electrostatic precipitators (Fig. 1). They have been in use over decades and have proved to be an effective way of collecting and removing particles from exhaust gases – the effectiveness is grater than 99%.

The principle of electrostatic precipitation is to separate the suspended particles from the exhaust gas by means of electric forces. First the particles are electrically charged, and then collected on the electrodes, where they are removed using a rapping system to be finally thrown into the external bin.

From the schematic description of the process it can be seen that the effectiveness of the electrostatic precipitation depends on many factors and

* *University of Bielsko-Biała, ul. Willowa 2, 43-309 Bielsko-Biała, Poland; email: i.adamiec@ath.eu*

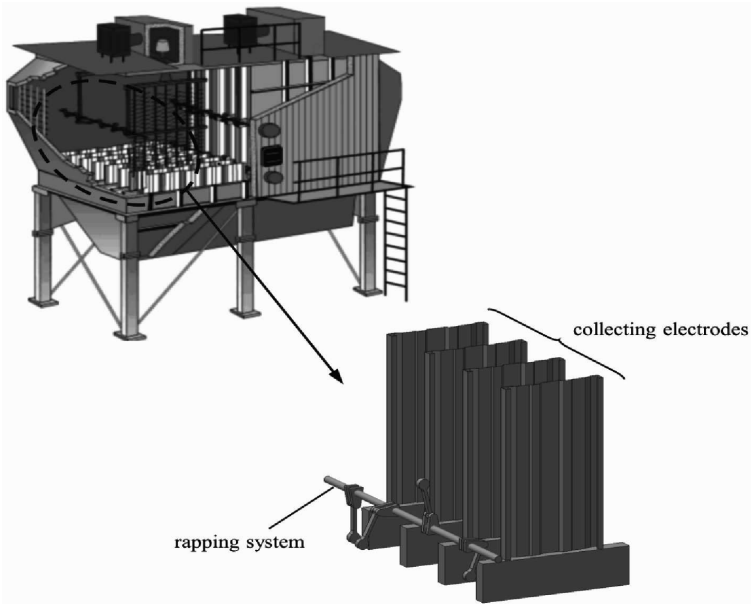

Fig. 1. Electrostatic precipitator and the system of collecting electrodes

the analysis of its performance requires interdisciplinary knowledge. Much research is devoted to electric aspects of the whole process [1-3] as well as particle migration and separation [4,5].

Periodic vibrations caused by the rapping system are responsible for proper cleaning of the dust from the collecting electrodes. Geometrical features of the electrodes, such as shape, length and thickness as well as the force impact caused by the beater, have an influence on tangent and normal accelerations of vibrations propagated over the collecting plates. This process in turn has an essential influence on the quality of particle collection on the plates. Modelling and analysis of those vibrations is the subject of this paper.

Analysis of the collecting electrodes with regard to their shape and dimensions requires not only advanced methods of modelling, but also sophisticated numerical methods for solving the equations of motion. The most popular method used for modeling complicated shapes is the finite element method [6] implemented in commercial software packages. The models formulated have a large number of degrees of freedom. Despite the existing commercial software, there are still problems for the solution of which it is profitable to create less sophisticated yet more specific programmes and algorithms of ones own. This is the case when modelling the collecting electrodes of electrostatic precipitators. The paper will present the hybrid

method of modelling the collecting electrodes and its application to dynamic analysis of the rapping system.

2. Model of the system

The rapping system consists of a set of collecting electrodes hanging on a suspension bar. At the bottom, the electrodes are braced together in a brushing bar, at the end of which there is an anvil (Fig. 2).

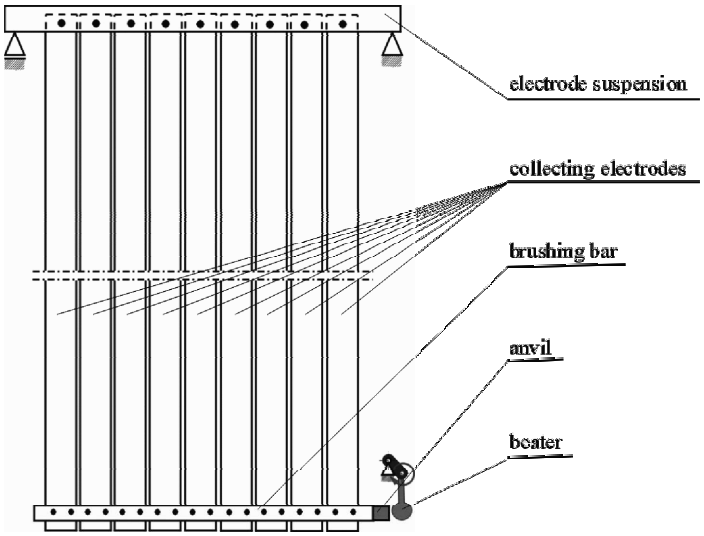

Fig. 2. The rapping system

The vibrations in the system are excited by means of a beater which periodically hits the anvil. The system is divided into subsystems which are: the top and bottom beams, and the collecting plates. Usually, there are nine collecting plates in one section of the rapping system, however, the number of active plates considered can vary between one and nine. The beams are discretised by means of the rigid finite element method [7], while the plates are modeled using the hybrid finite element method.

2.1. Models of the beams

The rigid finite element method is especially suitable for modelling beam-like links. The detailed description of the method is presented in [7,8]. There is one connection of the suspension bar with each plate and two connections of the plate with the brushing bar.

The number of elements into which the beams are discretised may be different for both beams. If p is the number of plates and a is the length

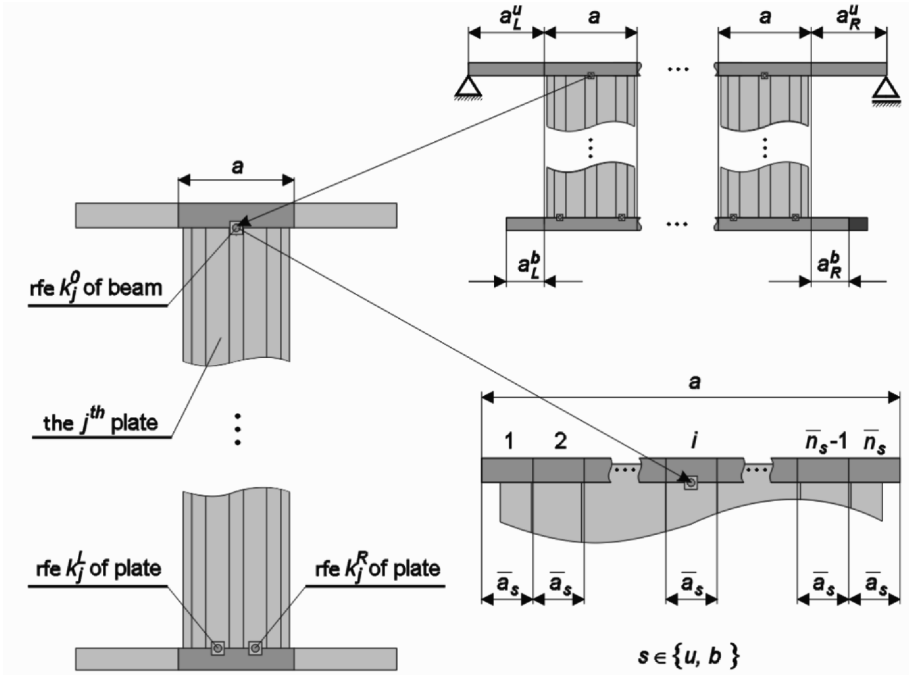

Fig. 3. Connections between the beams and the j-th plate

of a section of the beam respective to a single plate (all plates in a rapping system are usually the same) (Fig. 3), then in the primary division the length of rigid elements is as follows:

$$\begin{cases} d_0^s = a_L^s + \dfrac{\bar{a}_s}{2} \\ d_i^s = \bar{a}_s \qquad \text{for } i = 1, ..., p_s - 1 \\ d_{p_s}^s = \dfrac{\bar{a}_s}{2} + a_R^s \end{cases} \tag{1}$$

where: $\bar{a}_s = \dfrac{a}{n_s}, s \in \{u, b\}$, u, b means upper or bottom beam respectively, $p_s = n_s p$.

Following the idea of the rigid finite element method, the secondary division consists in placing spring-damping elements (sde) in the mass centres of the elements from the primary division and thus obtaining the rigid finite

elements (rfe), with the length equal to:

$$\begin{cases} l_0^s = \dfrac{d_0^s}{2} \\ l_i^s = \dfrac{d_{i-1}^s + d_i^s}{2} \qquad \text{for } i = 1, ..., p_s - 1 \\ l_{p_s}^s = \dfrac{d_{p_s}^s}{2} \end{cases} \tag{2}$$

For this analysis, it is assumed that both beams have the same shape of cross-section apart from the part of the bottom beam where the anvil is. This permissible simplification can be easily omitted. The supplementary box cross-section of beams is chosen as a result of analysis carried out by means of the finite element method. Geometrical parameters (Fig. 4) of the supplementary cross-section exactly reflect mass and stiffness parameters of the real beams. The coefficients of spring-damping elements can be calculated in the way described in [8].

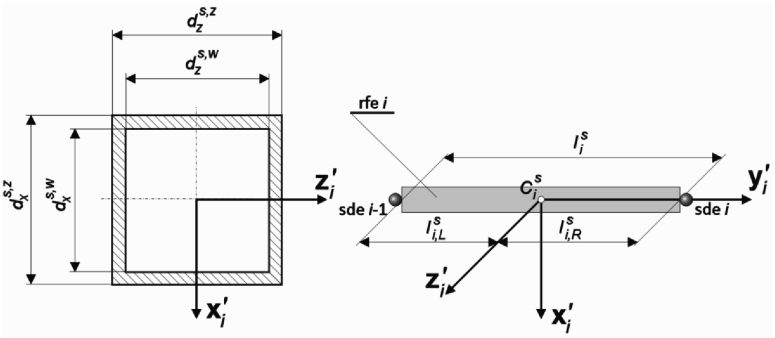

Fig. 4. Cross-section of the supplementary beam and parameters of rfes

The axes of the local coordinate system assigned to each rfe before deformation are parallel to the axes of the global reference system, and are the main central inertial axes of the element. Thus, the mass matrix of the element is diagonal and takes the following form:

$$\mathbf{M}_i^s = diag\left\{ m_i^s \quad m_i^s \quad m_i^s \quad I_{i,x}^s \quad I_{i,y}^s \quad I_{i,z}^s \right\} \tag{3}$$

where: $m_i^s = \rho l_i^s A^s$ is the mass of $i-$th rfe, A^s is the cross-section area,

$$I_{i,x}^s = m_i^s \left[\frac{\left(l_i^s\right)^2}{12} + \frac{I_x^s}{A^s} \right], \quad I_{i,y}^s = \frac{m_i^s}{A^s} \left[I_x^s + I_z^s \right], \quad I_{i,z}^s = m_i^s \left[\frac{\left(l_i^s\right)^2}{12} + \frac{I_z^s}{A^s} \right],$$

I_x^s, I_z^s are inertial moments of the cross-section of the beam.

The vector of generalised coordinates of rfe i is as follows:

$$\mathbf{q}_i^s = \left[\begin{array}{cccccc} \tilde{x}_i^s & \tilde{y}_i^s & \tilde{z}_i^s & \tilde{\varphi}_i^s & \tilde{\theta}_i^s & \tilde{\psi}_i^s \end{array} \right]^T \tag{4}$$

where: $\tilde{x}_i^s, \tilde{y}_i^s, \tilde{z}_i^s$ are displacements of the mass centre S_i^s of rfe,

$\tilde{\varphi}_i^s, \tilde{\theta}_i^s, \tilde{\psi}_i^s$ are the angles of rotations.

The kinetic energy of the i-th rfe is calculated according to the formula:

$$E_i^s = \frac{1}{2} \left[\dot{\mathbf{q}}_i^s \right]^T \mathbf{M}_i^s \dot{\mathbf{q}}_i^s \tag{5}$$

Since the elements of $\mathbf{M}_i^s$ are constant the Lagrange operator takes the form:

$$\varepsilon_{\mathbf{q}_i^s} = \mathbf{M}_i^s \ddot{\mathbf{q}}_i^s \tag{6}$$

where $\varepsilon_{\mathbf{q}_i^s} = \dfrac{d}{dt} \dfrac{\partial E_i^s}{\partial \dot{\mathbf{q}}_i^s} - \dfrac{\partial E_i^s}{\partial \mathbf{q}_i^s}$.

The derivative of the potential energy of gravity forces is calculated as:

$$\frac{\partial V_{g,i}^s}{\partial \mathbf{q}_i^s} = \left[\begin{array}{cccccc} -m_i^s g & 0 & 0 & 0 & 0 & 0 \end{array} \right]^T = \mathbf{G}_i^s \tag{7}$$

The energy of spring deformation can be presented in the form:

$$\mathbf{V}_{e,i}^s = \frac{1}{2} \left(\mathbf{\Delta}_i^s \right)^T \mathbf{C}_i^s \mathbf{\Delta}_i^s \tag{8}$$

where: $\mathbf{C}_i^s = diag \left\{ \begin{array}{ccc} c_{i,1}^s & \cdots & c_{i,6}^s \end{array} \right\}$,

$c_{i,j}^s$ are the stiffness coefficients,

$\mathbf{\Delta}_i^s$ is the deformation of sde i.

Having used notations from Fig. 4.b), after necessary transformations the derivatives of spring energy with respect to the generalised coordinates can be presented in the form:

$$\frac{\partial \mathbf{V}_{e,i}^s}{\partial \mathbf{q}_i^s} = -\left(\mathbf{H}_{i,1}^s \right)^T \mathbf{C}_i^s \left[\mathbf{H}_{i,2}^s \mathbf{q}_{i+1}^s - \mathbf{H}_{i,1}^s \mathbf{q}_i^s \right] = \mathbf{C}_{i,LL}^s \mathbf{q}_i^s + \mathbf{C}_{i,LR}^s \mathbf{q}_{i+1}^s \tag{9.1}$$

$$\frac{\partial \mathbf{V}_{e,i}^s}{\partial \mathbf{q}_{i+1}^s} = \left(\mathbf{H}_{i,2}^s \right)^T \mathbf{C}_i^s \left[\mathbf{H}_{i,2}^s \mathbf{q}_{i+1}^s - \mathbf{H}_{i,1}^s \mathbf{q}_i^s \right] = \mathbf{C}_{i,RL}^s \mathbf{q}_i^s + \mathbf{C}_{i,RR}^s \mathbf{q}_{i+1}^s \tag{9.2}$$

where: $\mathbf{C}_{i,LL}^s = \left(\mathbf{H}_{i,1}^s \right)^T \mathbf{C}_i^s \mathbf{H}_{i,1}^s$, $\quad \mathbf{C}_{i,LR}^s = -\left(\mathbf{H}_{i,1}^s \right)^T \mathbf{C}_i^s \mathbf{H}_{i,2}^s$,

$$\mathbf{C}^s_{i,RL} = -\left(\mathbf{H}^s_{i,2}\right)^T \mathbf{C}^s_i \mathbf{H}^s_{i,1}, \qquad \mathbf{C}^s_{i,RR} = \left(\mathbf{H}^s_{i,2}\right)^T \mathbf{C}^s_i \mathbf{H}^s_{i,2},$$

$$\mathbf{H}^s_{i,1} = \begin{bmatrix} \mathbf{I} & \mathbf{S}^s_{i,R} \\ \mathbf{0} & \mathbf{I} \end{bmatrix}, \qquad \mathbf{H}^s_{i,2} = \begin{bmatrix} \mathbf{I} & \mathbf{S}^s_{i+1,L} \\ \mathbf{0} & \mathbf{I} \end{bmatrix},$$

$$\mathbf{S}^s_{i,R} = \begin{bmatrix} 0 & 0 & -l^s_{i,R} \\ 0 & 0 & 0 \\ l^s_{i,R} & 0 & 0 \end{bmatrix}, \qquad \mathbf{S}^s_{i+1,L} = \begin{bmatrix} 0 & 0 & l^s_{i+1,L} \\ 0 & 0 & 0 \\ -l^s_{i+1,L} & 0 & 0 \end{bmatrix}.$$

Kinetic and potential energies of the beams are the sum of energies of all rfes:

$$E^s = \sum_{i=0}^{p_s+1} E^s_i \tag{10.1}$$

$$V^s_g = \sum_{i=0}^{p_s+1} V^s_{g,i} \tag{10.2}$$

and the potential energy of spring deformation is the sum of energies of sdes $0 \div p_s$:

$$V^s_e = \sum_{i=0}^{p_s} V^s_{e,i} \tag{11}$$

The vector of generalised coordinates of a beam can be presented as:

$$\mathbf{q}^s = \begin{bmatrix} \mathbf{q}^s_0 \\ \vdots \\ \mathbf{q}^s_i \\ \vdots \\ \mathbf{q}^s_{p_s+1} \end{bmatrix} \tag{12}$$

So finally, the following can be written:

$$\frac{d}{dt}\frac{\partial E^s}{\partial \dot{\mathbf{q}}^s} - \frac{\partial E^s}{\partial \mathbf{q}^s} + \frac{\partial \left(V^s_g + V^s_e\right)}{\partial \mathbf{q}^s} = \mathbf{M}^s \ddot{\mathbf{q}}^s + \mathbf{K}^s \mathbf{q}^s + \mathbf{G}^s \tag{13}$$

where:

$$\mathbf{M}^s = \begin{bmatrix} \mathbf{M}^s_0 & \cdots & \mathbf{0} & \cdots & \mathbf{0} \\ \vdots & & \vdots & & \vdots \\ \mathbf{0} & \cdots & \mathbf{M}^s_i & \cdots & \mathbf{0} \\ \vdots & & \vdots & & \vdots \\ \mathbf{0} & \cdots & \mathbf{0} & \cdots & \mathbf{M}^s_{p_s+1} \end{bmatrix},$$

$$\mathbf{K}^s = \begin{bmatrix} \mathbf{K}^s_{0,0} & \mathbf{K}^s_{0,1} & \mathbf{0} & \cdots & \mathbf{0} & \mathbf{0} & \mathbf{0} & \mathbf{0} & \mathbf{0} & \cdots & \mathbf{0} & \mathbf{0} & \mathbf{0} \\ \vdots & \vdots & \vdots & & \vdots & \vdots & \vdots & \vdots & \vdots & & \vdots & \vdots & \vdots \\ \mathbf{0} & \mathbf{0} & \mathbf{0} & \cdots & \mathbf{0} & \mathbf{K}^s_{i,i-1} & \mathbf{K}^s_{i,i} & \mathbf{K}^s_{i,i+1} & \mathbf{0} & \cdots & \mathbf{0} & \mathbf{0} & \mathbf{0} \\ \vdots & \vdots & \vdots & & \vdots & \vdots & \vdots & \vdots & \vdots & & \vdots & \vdots & \vdots \\ \mathbf{0} & \mathbf{0} & \mathbf{0} & \cdots & \mathbf{0} & \mathbf{0} & \mathbf{0} & \mathbf{0} & \mathbf{0} & \cdots & \mathbf{0} & \mathbf{K}^s_{p_s+1,p_s} & \mathbf{K}^s_{p_s+1,p_s+1} \end{bmatrix},$$

$$\mathbf{G}^s = \begin{bmatrix} \mathbf{G}^s_0 \\ \vdots \\ \mathbf{G}^s_i \\ \vdots \\ \mathbf{G}^s_{p_s+1} \end{bmatrix}, \qquad \begin{array}{l} \mathbf{K}^s_{0,0} = \mathbf{C}^s_{0,LL}, \mathbf{K}^s_{0,1} = \mathbf{C}^s_{0,LR} \\ \mathbf{K}^s_{i,i-1} = \mathbf{C}^s_{i-1,RL}, \mathbf{K}^s_{i,i} = \mathbf{C}^s_{i-1,RR} + \mathbf{C}^s_{i,LL}, \mathbf{K}^s_{i,i+1} = \mathbf{C}^s_{i,LR} \\ \mathbf{K}^s_{p_s+1,p_s} = \mathbf{C}^s_{p_s,RL}, \mathbf{K}^s_{p_s+1,p_s+1} = \mathbf{C}^s_{p_s,RR} \end{array}.$$

Thus, the motion of beams is described by the following number of generalised coordinates:

$$n^s_{dof} = 6\,(p_s + 2) \tag{14}$$

The upper beam is connected with the base, and this connection has to be taken into account when deriving the equations of motion. The connection is modelled by means of spring elements as in Fig. 5.

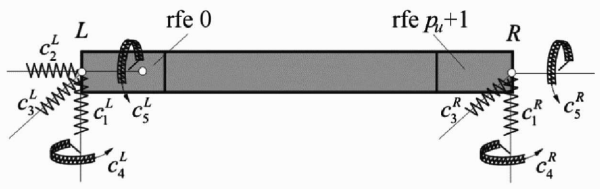

Fig. 5. Connection of the suspension beam with the base

The energy of spring deformation of those elements can be calculated as:

$$\mathbf{V}_L = \frac{1}{2}\boldsymbol{\Delta}_L^T \mathbf{C}_L \boldsymbol{\Delta}_L \tag{15.1}$$

$$\mathbf{V}_R = \frac{1}{2}\boldsymbol{\Delta}_R^T \mathbf{C}_R \boldsymbol{\Delta}_R \tag{15.2}$$

where: $\mathbf{C}_L = diag\left\{c_i^L\right\}$, $\mathbf{C}_R = diag\left\{c_i^R\right\}$, $i = 1, \ldots 6$

$\boldsymbol{\Delta}_L, \boldsymbol{\Delta}_R$ vectors of deformations at L and R.

It is assumed that $c_6^L = c_2^R = c_6^R = 0$. Values $\boldsymbol{\Delta}_L, \boldsymbol{\Delta}_R$ can be calculated as:

$$\boldsymbol{\Delta}_L = \mathbf{H}_L \mathbf{q}_0^u \tag{16.1}$$

$$\boldsymbol{\Delta}_R = \mathbf{H}_R \mathbf{q}_{p+1}^u \tag{16.2}$$

where:

$$\mathbf{H}_L = \begin{bmatrix} \mathbf{I} & \mathbf{S}_L \\ \mathbf{0} & \mathbf{I} \end{bmatrix}, \quad \mathbf{H}_R = \begin{bmatrix} \mathbf{I} & \mathbf{S}_R \\ \mathbf{0} & \mathbf{I} \end{bmatrix},$$

$$\mathbf{S}_L = \begin{bmatrix} 0 & 0 & \frac{l^u_0}{2} \\ 0 & 0 & 0 \\ -\frac{l^u_0}{2} & 0 & 0 \end{bmatrix}, \quad \mathbf{S}_R = \begin{bmatrix} 0 & 0 & -\frac{l^u_{p_t+1}}{2} \\ 0 & 0 & 0 \\ \frac{l^u_{p_t+1}}{2} & 0 & 0 \end{bmatrix}.$$

Thus, the following is achieved:

$$\frac{\partial \mathbf{V}_L}{\partial \mathbf{q}^u_0} = \mathbf{K}_L \mathbf{q}^u_0 \tag{17.1}$$

$$\frac{\partial \mathbf{V}_R}{\partial \mathbf{q}^u_{p_t+1}} = \mathbf{K}_R \mathbf{q}^u_{p_t+1} \tag{17.2}$$

Matrices $\mathbf{K}_L$ and $\mathbf{K}_R$ have to be added to sub-matrices $\mathbf{K}^u_{0,0}$ and $\mathbf{K}^u_{p_u+1,p_u+1}$ in matrix $\mathbf{K}^u$.

As has been mentioned, the vibrations in the rapping system are excited when the beater hits the anvil. It is assumed that the impulse of a force (Fig. 6) is modelled as a central, straight stroke of force $\mathbf{F} = \begin{bmatrix} 0 & -S(t) & 0 \end{bmatrix}^T$.

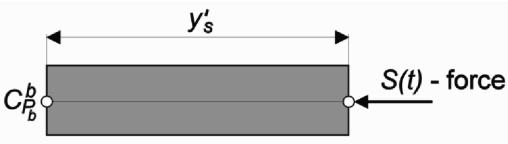

Fig. 6. Force acting on the anvil

The coordinates of the point where the force acts, can be calculated according to the formula:

$$\mathbf{r}_S = \mathbf{r}^b_{C,p_b+1} + \mathbf{U}^b_{p_b+1}(\tilde{\mathbf{r}}_S)\,\mathbf{q}^b_{p_b+1} \tag{18}$$

where: $\tilde{\mathbf{r}}_S = \begin{bmatrix} x'_S & y'_S & z'_S \end{bmatrix}^T = \begin{bmatrix} 0 & -y'_S & 0 \end{bmatrix}^T$,

$$\mathbf{U}^b_{p_b+1} = \begin{bmatrix} 1 & 0 & 0 & 0 & z'_S & -y'_S \\ 0 & 1 & 0 & -x'_S & 0 & z'_S \\ 0 & 0 & 1 & y'_S & -z'_S & 0 \end{bmatrix}.$$

The generalised forces can be calculated as:

$$\left[\mathbf{Q}^{(S)}_{p_b+1}\right]^T = \mathbf{F}^T \frac{\partial \mathbf{r}_S}{\partial \mathbf{q}^b_{p_b+1}} = \mathbf{F}^T \mathbf{U}^b_{p_b+1} \tag{19}$$

which leads to the following:

$$\left[\mathbf{Q}^{(S)}_{p_b+1}\right]^T = \begin{bmatrix} 0 & -S & 0 \end{bmatrix} \begin{bmatrix} 1 & 0 & 0 & 0 & 0 & -y'_S \\ 0 & 1 & 0 & 0 & 0 & 0 \\ 0 & 0 & 1 & y'_S & 0 & 0 \end{bmatrix} = \begin{bmatrix} 0 & -S & 0 & 0 & 0 & 0 \end{bmatrix} \tag{20}$$

2.2. Model of the plates

The collecting electrodes of sigma shape are considered (Fig. 7). The length of the electrodes can vary between 10 and 15 meters. The natural method of discretisation of a single plate results from its shape. The rigid finite element method is not suitable for modelling shell structures; thus a hybrid finite element method [9] is proposed.

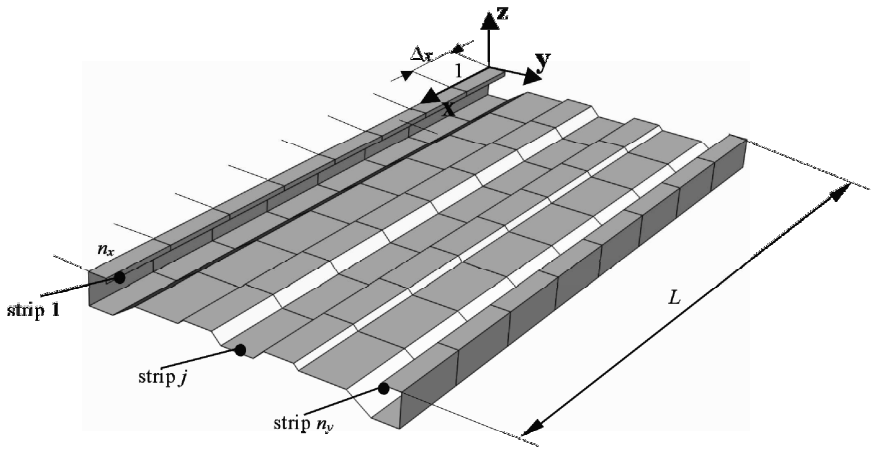

Fig. 7. Sigma electrode

This method combines the rigid finite element method with the classical finite element method. First, the finite element method is used for calculations of spring deformations and thus the stiffness matrix is formulated. Then the rigid finite element method is used for modelling mass properties of the system.

The local coordinate system is assigned to the plate as in Fig. 7. Discretisation of the plate into $n = n_x n_y$ elements is carried out in two steps. First,

using its natural shape, the plate is discretised into rectangular elements, called primary elements: there are n_x elements along the length of the plate, while the number of elements in direction of axis **y** $n_y = m$ results from the number of strips.

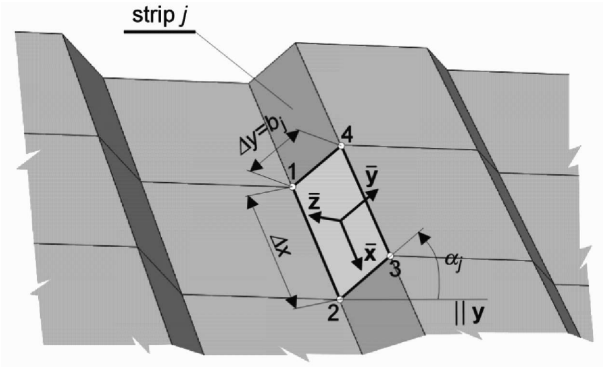

Fig. 8. Primary element (i,j)

The nodal displacements of the element (Fig. 8) are described by the vector:

$$\bar{\mathbf{q}}^s_{i,j} = \left[\bar{u}^s_{i,j}, \bar{v}^s_{i,j}, \bar{w}^s_{i,j}, \bar{\varphi}^s_{i,j}, \bar{\theta}^s_{i,j}, \bar{\psi}^s_{i,j}\right]^{\mathrm{T}} \text{ for} s = 1,2,3,4 \tag{21}$$

where: $\bar{u}^s_{i,j}, \bar{v}^s_{i,j}, \bar{w}^s_{i,j}$ are displacements of node s along $\bar{\mathbf{x}}, \bar{\mathbf{y}}, \bar{\mathbf{z}}$ axes respectively, $\bar{\varphi}^s_{i,j}, \bar{\theta}^s_{i,j}, \bar{\psi}^s_{i,j}$ are respective rotations.

It is assumed that:

– shield deformations are described by means of displacements $\bar{u}^s_{i,j}, \bar{v}^s_{i,j}$ and angle $\bar{\psi}^s_{i,j}$

– plate deformations are described by displacement $\bar{w}^s_{i,j}$ and angles $\bar{\varphi}^s_{i,j}, \bar{\theta}^s_{i,j}$.

The shape functions and respective angles are defined as follows:

$$\bar{u} = a^u_1 + a^u_2\bar{x} + a^u_3\bar{y} + a^u_4\bar{x}\bar{y} + a^u_5\bar{y}^2 + a^u_6\bar{x}\bar{y}^2 \tag{22.1}$$

$$\bar{v} = a^v_1 + a^v_2\bar{x} + a^v_3\bar{y} + a^v_4\bar{x}\bar{y} + a^v_5\bar{x}^2 + a^v_6\bar{x}^2\bar{y} \tag{22.2}$$

$$\begin{aligned}\bar{w} = {} & a^w_1 + a^w_2\bar{x} + a^w_3\bar{y} + a^w_4\bar{x}^2 + a^w_5\bar{x}\bar{y} + a^w_6\bar{y}^2 + a^w_7\bar{x}^3 + \\ & + a^w_8\bar{x}^2\bar{y} + a^w_9\bar{x}\bar{y}^2 + a^w_{10}\bar{y}^3 + a^w_{11}\bar{x}^3\bar{y} + a^w_{12}\bar{x}\bar{y}^3\end{aligned} \tag{22.3}$$

$$\bar{\varphi} = \frac{\partial\bar{w}}{\partial\bar{y}} \tag{22.4}$$

$$\bar{\theta} = -\frac{\partial\bar{w}}{\partial\bar{x}} \tag{22.5}$$

$$\bar{\psi} = \frac{1}{2}\left(\frac{\partial \bar{v}}{\partial \bar{x}} - \frac{\partial \bar{u}}{\partial \bar{y}}\right) \tag{22.6}$$

The energy of spring deformations, after necessary calculations can be presented in the form:

$$E^s_{i,j} = \tfrac{1}{2}\left[\bar{\mathbf{q}}^{1\ T}_{i,j} \quad \bar{\mathbf{q}}^{2\ T}_{i,j} \quad \bar{\mathbf{q}}^{3\ T}_{i,j} \quad \bar{\mathbf{q}}^{4\ T}_{i,j}\right]\begin{bmatrix} \mathbf{C}^{i,j}_{11} & \mathbf{C}^{i,j}_{12} & \mathbf{C}^{i,j}_{13} & \mathbf{C}^{i,j}_{14} \\ \mathbf{C}^{i,j}_{21} & \mathbf{C}^{i,j}_{22} & \mathbf{C}^{i,j}_{23} & \mathbf{C}^{i,j}_{24} \\ \mathbf{C}^{i,j}_{31} & \mathbf{C}^{i,j}_{32} & \mathbf{C}^{i,j}_{33} & \mathbf{C}^{i,j}_{34} \\ \mathbf{C}^{i,j}_{41} & \mathbf{C}^{i,j}_{42} & \mathbf{C}^{i,j}_{43} & \mathbf{C}^{i,j}_{44} \end{bmatrix}\begin{bmatrix} \bar{\mathbf{q}}^{1}_{i,j} \\ \bar{\mathbf{q}}^{2}_{i,j} \\ \bar{\mathbf{q}}^{3}_{i,j} \\ \bar{\mathbf{q}}^{4}_{i,j} \end{bmatrix} = \tfrac{1}{2}\bar{\mathbf{q}}^{T}_{i,j}\mathbf{C}^{i,j}\bar{\mathbf{q}}_{i,j} \tag{23}$$

where: $\bar{\mathbf{q}}^s_{i,j}$, $s = 1...4$ defined in (21),

$\mathbf{C}^{i,j}_{rs}$, $r, s = 1...4$ are 6×6 stiffness matrices, whose components are ordered according to the nodal coordinates in vector $\bar{\mathbf{q}}^s_{i,j}$.

It should be noted that for defined physical parameters of plates E, υ, α, h, the stiffness matrices of the elements depend only on dimensions Δx and $\Delta y = b_j$ so they are calculated only for $j = 1, \ldots, n_y$.

Generalised coordinates defined in (21) need to be expressed in the coordinate system with axes parallel to the global coordinate system and thus the following transformation takes place:

$$\mathbf{q}_{i,j} = \begin{bmatrix} \bar{\mathbf{R}}_{\alpha_j} & \mathbf{0} \\ \mathbf{0} & \bar{\mathbf{R}}_{\alpha_j} \end{bmatrix}\bar{\mathbf{q}}_{i,j} \tag{24}$$

where:

$$\bar{\mathbf{R}}_{\alpha_j} = \begin{bmatrix} 1 & 0 & 0 \\ 0 & \cos\alpha_j & -\sin\alpha_j \\ 0 & \sin\alpha_j & \cos\alpha_j \end{bmatrix}.$$

Having calculated energy of spring deformation, we perform a secondary division of the plate. This is an idea taken from the rigid finite element method in which rigid finite elements reflect inertial features, while connecting spring-damping elements reflect elastic features of the system. Since in the hybrid finite element the elastic deformations are described as above, only the mass matrix has to be calculated. To this end each element from the primary division is divided into four equal sub-elements (Fig. 9).

Then the rigid finite elements (rfe) are formed combining neighboring parts of primary elements in such a way that two parts of the same primary element do not belong to the same rfe. Finally, the plate can be treated as a system of $n = (n_x + 1)\,m = (n_x + 1)\left(n_y + 1\right)$ rfes consisting of one, two or four sub-elements of different primary elements.

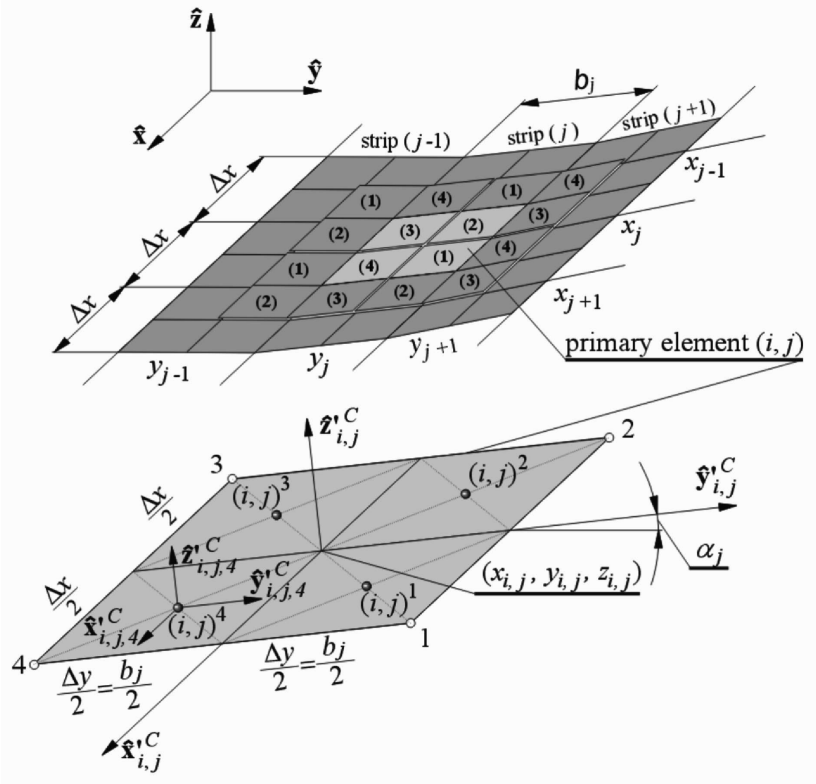

Fig. 9. Primary division of a plate and division of primary element (i, j) into four sub elements $(i, j)^1$, $(i, j)^2$, $(i, j)^3$, $(i, j)^4$

The vector of generalised coordinates of each rfe k includes three displacements and three rotations and is given in the following form:

$$\tilde{\mathbf{q}}_k^{rfe} = \left[\Delta\tilde{x}_k, \Delta\tilde{y}_k, \Delta\tilde{z}_k, \tilde{\varphi}_k^x, \tilde{\varphi}_k^y, \tilde{\varphi}_k^z\right]^T \tag{25}$$

When vibrations of collecting plates are considered, it can be assumed that angles $\varphi_k^x, \varphi_k^y, \varphi_k^z$ are small. Thus, when coordinates (x', y', z') of a point are known in the local system of rfe k, then its coordinates in the global coordinate system can be calculated as follows:

$$\mathbf{r} = \mathbf{r}_k^{rfe} + \bar{\mathbf{R}}_{\beta_K}\left[\mathbf{U}\tilde{\mathbf{q}}_k^{rfe} + \mathbf{r}'\right] \tag{26}$$

where: $\mathbf{r}' = [x', y', z']^T$,

$\mathbf{U}$ is defined in (18),

$\mathbf{r}_k^{rfe}$ is the vector of coordinates of the mass center of rfe k,

$\bar{\mathbf{R}}_{\beta_k}$ is defined in (24),

β_k is the angle resulting from the fact, that axes of the local coordinate system of rfe are main central inertial axes of the element.

Using the standard RFE approach the diagonal mass matrix of rfe k can be formulated:

$$\mathbf{M}_k = diag\left\{m_k, m_k, m_k, I_k^x, I_k^y, I_k^z\right\} \tag{27}$$

And since the generalised coordinates of rfes are independent, the mass matrix of a system of n rfes takes the form:

$$\mathbf{M} = diag\left\{\mathbf{M}_1, \mathbf{M}_2, ..., \mathbf{M}_n\right\} \tag{28}$$

This is a diagonal matrix with constant coefficients. Displacements of rfes are described by means of displacements of primary elements.

In order to formulate the stiffness matrix for the whole electrode, the displacements of primary elements need to be expressed in terms of generalised coordinates of the rigid finite elements.

To this end, the coordinates of nodes of primary element (i, j) are first expressed in the global coordinate system and then, after some transformations the vector of generalised coordinates of the nodes can be presented in the following form:

$$\mathbf{q}_{i,j} = \begin{bmatrix} \bar{\mathbf{R}}_{\alpha_j}^T \bar{\mathbf{R}}_{\beta_k} \mathbf{U}(\mathbf{r'}_{i,j}^s) \\ \mathbf{R}_{\alpha_j}^T \bar{\mathbf{R}}_{\beta_k} \mathbf{S} \end{bmatrix} \mathbf{q}_k^{rfe} \tag{29}$$

where: $\mathbf{r'}_{i,j}^s$ are coordinates of a node of primary element (i,j) in local system of rfe k,

$\mathbf{U}$ is defined in (18) for x, y, z coordinates of vector $\mathbf{r'}_{i,j}^s$,

$$\mathbf{S} = \begin{bmatrix} 0 & 0 & 0 & 1 & 0 & 0 \\ 0 & 0 & 0 & 0 & 1 & 0 \\ 0 & 0 & 0 & 0 & 0 & 1 \end{bmatrix}.$$

Such a procedure have to be carried out for each collecting plate. In order to formulate the equations of motion of the system, mass and stiffness matrices will have a superscript denoting the number of the plate. Stiffness matrix $\mathbf{K}$ of the plate is composed of matrices defined in (24).

2.3. Equations of motion

The equations of motion for the system can be written in the form:

$$\mathbf{M}^u \ddot{\mathbf{q}}^u + \mathbf{K}^u \mathbf{q}^u = -\mathbf{G}^u \tag{30.1}$$

$$\mathbf{M}^j\ddot{\mathbf{q}}^j + \mathbf{K}^j\mathbf{q}^j = -\mathbf{G}^j,\ j = 1, ..., n_p \tag{30.2}$$

$$\mathbf{M}^b\ddot{\mathbf{q}}^b + \mathbf{K}^b\mathbf{q}^b = -\mathbf{G}^b + \mathbf{f}^b(S) \tag{30.3}$$

where n_p is the number of active plates,
$\mathbf{M}^u, \mathbf{K}^u, \mathbf{M}^b, \mathbf{K}^b$ are mass and stiffness matrices for the top and bottom beams respectively as defined in subsection (2.1),
$\mathbf{M}^j, \mathbf{K}^j$ are mass and stiffness matrices for each plate defined in section 2.2 ,
$\mathbf{G}^u, \mathbf{G}^j, \mathbf{G}^b$ are vectors resulting from the gravity forces for the upper beam, the plates and the bottom beam respectively,

$\mathbf{f}^b = \begin{bmatrix} \mathbf{0} \\ \vdots \\ \mathbf{0} \\ \vdots \\ \mathbf{Q}^{(S)T}_{p_b+1} \end{bmatrix}$, $\mathbf{Q}^{(S)T}_{p_b+1}$ is defined in (20).

The equations of motion need to be completed with components describing the connections between the subsystems. As was mentioned, there is one connection between the upper beam and the plate, and two connections between the plate and the bottom beam. These connections are modelled by means of elastic elements sde_E between two rigid bodies. Such an approach enables us to replace formulation of constraint equations by calculation of the energy of spring deformation, which can be written in the form:

$$V_E = \tfrac{1}{2}\tilde{\mathbf{\Delta}}_E^T\mathbf{C}_E\tilde{\mathbf{\Delta}}_E \tag{31}$$

where: $\mathbf{C}_E = diag\left\{c_E^x, c_E^y, c_E^z, c_E^\varphi, c_E^\theta, c_E^\psi\right\}$,

$c_E^x, c_E^y, c_E^z, c_E^\varphi, c_E^\theta, c_E^\psi$ are stiffness coefficients of the elastic connection,

$\tilde{\mathbf{\Delta}}_E$ is the vector of relative displacement between the elements connected by sde_E expressed in the local coordinate system $\{E\}$.

Since the energy of spring deformation of the connection depends on the generalised coordinates of the two bodies connected by this element, the derivatives of the energy with respect to those coordinates need be calculated as:

$$\frac{\partial V_E}{\partial \tilde{\mathbf{q}}^{(l)}} = \mathbf{C}_{ll}^{(E)}\tilde{\mathbf{q}}^{(l)} + \mathbf{C}_{lr}^{(E)}\tilde{\mathbf{q}}^{(r)} \tag{32.1}$$

$$\frac{\partial V_E}{\partial \tilde{\mathbf{q}}^{(r)}} = \mathbf{C}_{rl}^{(E)} \tilde{\mathbf{q}}^{(l)} + \mathbf{C}_{rr}^{(E)} \tilde{\mathbf{q}}^{(r)} \tag{32.2}$$

where: r, l are the indexes of right and left body in the connection,

$\mathbf{C}_{ll}^{(E)}, \mathbf{C}_{rl}^{(E)}, \mathbf{C}_{rr}^{(E)}$ are stiffness matrices calculated after some necessary transformations in which the coordinates are expressed in the global coordinate system.

The elastic element is universal since it can represent rotary, translation or a spherical bearing according to values of stiffness coefficients assumed.

For numerical calculations values of $10^{12} N/m$ has been assumed to translational and $10^{9} Nm/rad$ rotational coefficients.

3. Numerical simulations

Free vibrations of a simple square plate calculated using the hybrid element method and their comparison with an analytical solution, are presented in [8]. In addition, a model of a single sigma collecting electrode 15m long is derived, and free vibrations calculated using this model are compared with those obtained from ABAQUS and ANSYS. Table 1 presents the comparison the first ten frequencies of free vibrations, assuming that the electrode has been divided into n_x=60 segments and n_y=19 strips.

Table 1.

The comparison of frequencies of free vibrations for a SIGMA plate

Free vibrations	Method/package used		
	ANSYS	ABAQUS	Hybrid method
	Frequency of free vibrations [Hz]		
1	0,54	0,59	0,60
2	1,17	1,05	1,17
3	2,09	2,04	2,15
4	3,20	2,88	3,19
5	5,15	4,85	5,19
6	6,08	5,50	6,06
7	9,58	8,73	9,54
8	9,70	9,05	9,73
9	13,44	12,48	13,36
10	13,61	13,41	13,51

The frequencies of free vibrations obtained by means of the hybrid method differ by about 10% from those obtained using ANSYS and by about 5.5% in comparison with those obtained from ABAQUS. Comparison of the free vibrations of the sigma plate with a strip method, when spline functions of the third order are used in order to model deflections along the length of the plate, is presented in [10]. The strip method is also presented in [11]. Since the systems of equations of motion derived using both methods (the hybrid finite element method and the strip method) are very large, they require the use of efficient numerical procedures, which is discussed in [12]. Static analysis of the collecting electrodes is the subject of [13]. The results presented below are calculated for a system of three sigma electrodes 15 m long. The vibrations are caused by a force impulse shown in Fig. 10.

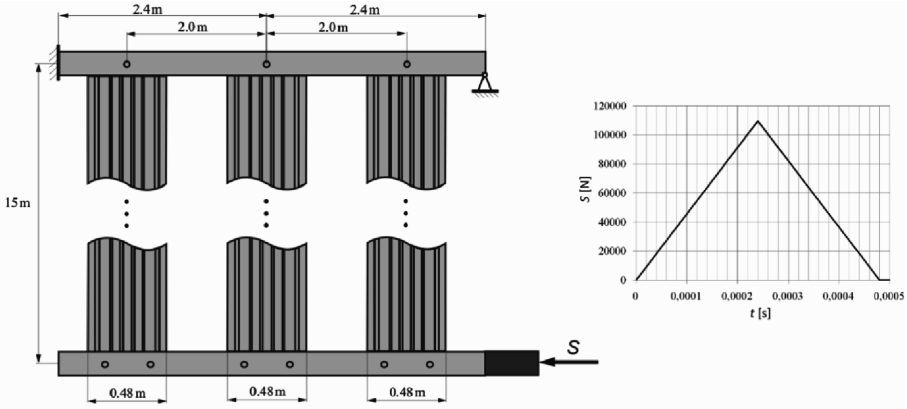

Fig. 10. The system of three collecting plates and the force impulse assumed

An influence of the number of elements into which a single plate is discretised is presented in Fig. 11 and 12.

The figures show the courses of components of accelerations calculated at different points of the plate: in the middle of the central plate 2m from the top beam and in half way along the plate close to the anvil. Convergence of results is obtained for n larger than 300.

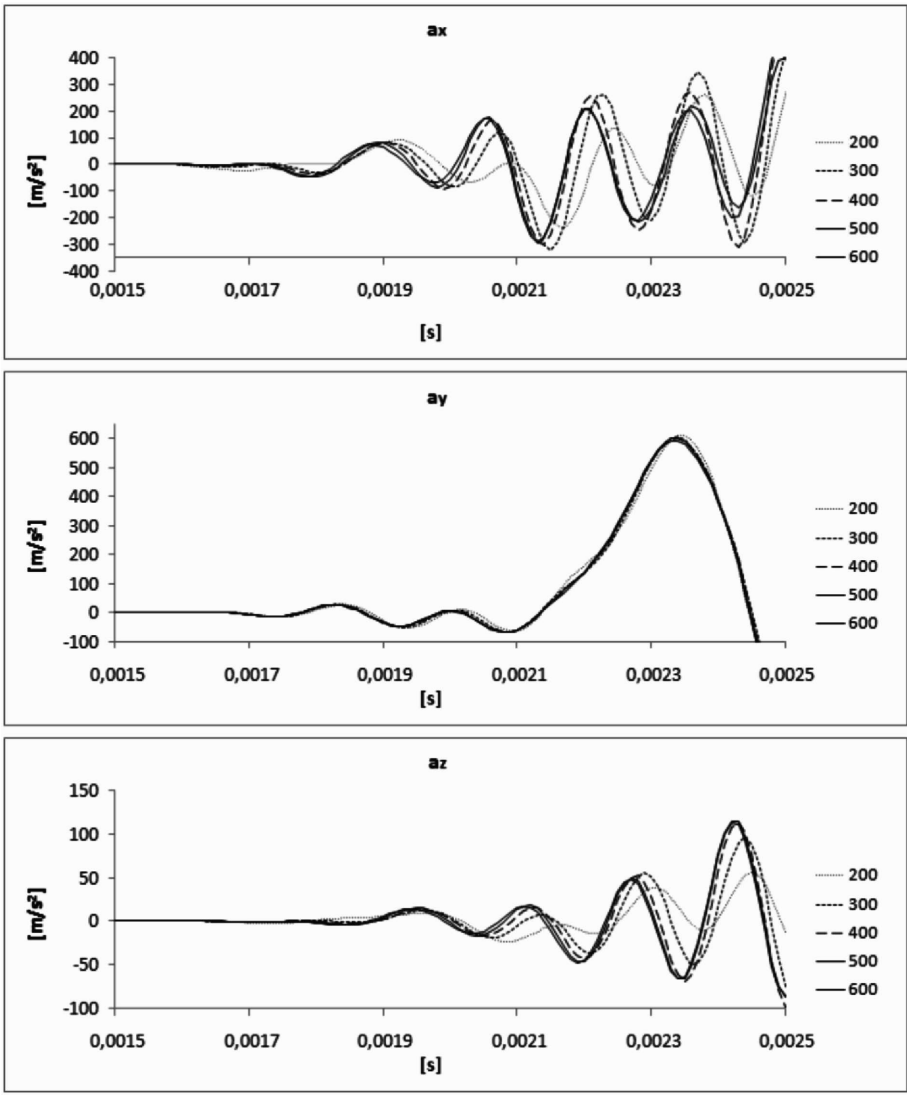

Fig. 11. Accelerations in **x,y,z** directions in the middle of the central plate

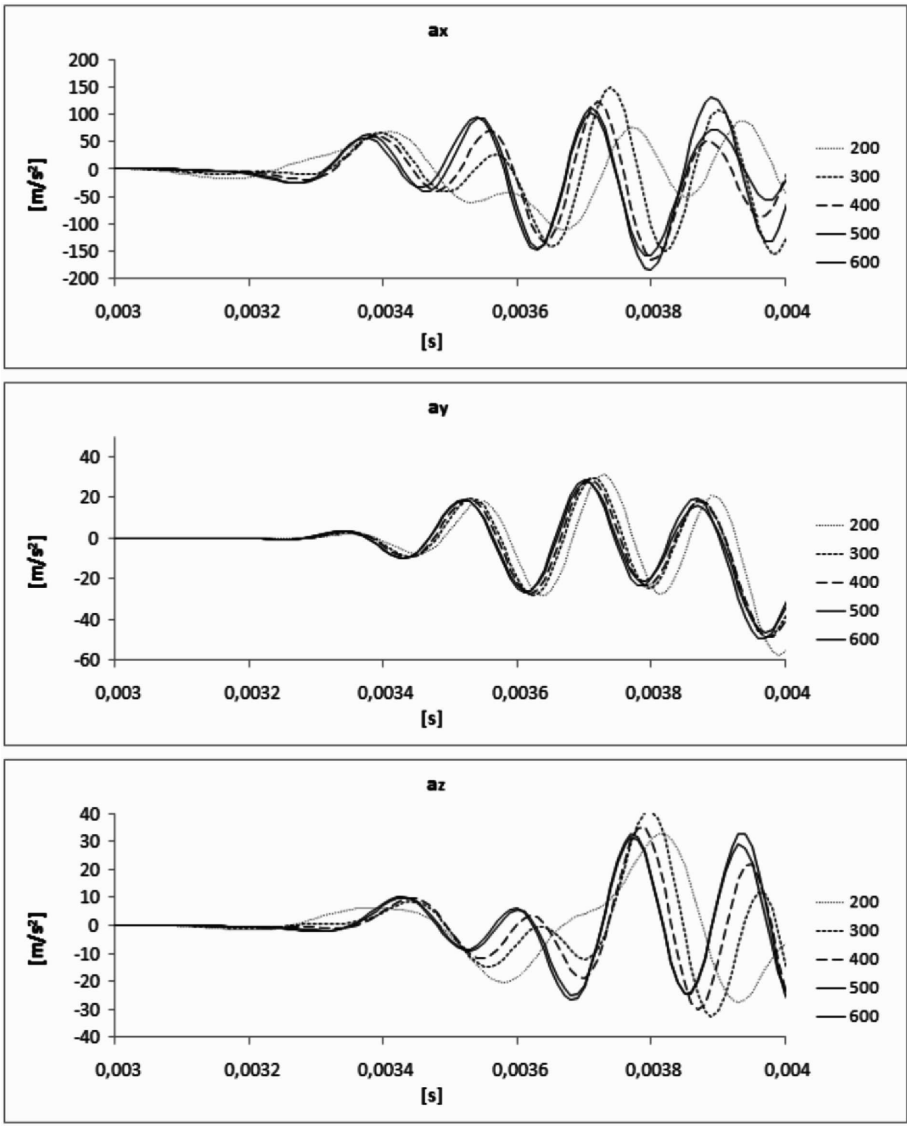

Fig. 12. Accelerations in **x,y,z** directions in the middle of the first plate

4. Final remarks

Accelerations of vibrations propagated in collecting electrodes are one of the essential factors influencing the effectiveness of cleaning the collecting electrodes and thus the effectiveness of electrostatic precipitation. A computer programme enabling dynamic analysis of the rapping system has been developed based on the model presented in the paper. The model uses the rigid finite element method for discretisation of the suspension of the electrodes and the brushing bar, and the hybrid finite element method for discretisation of the plates. In the hybrid method proposed, discretisation into rigid finite elements is the major task because the generalized coordinates describing the motion of the system are displacements and rotations of rfes in local coordinate systems. Motion of an rfe is limited only by the influence of primary elements, and thus when modelling connections of the SIGMA plate with the base or other components of the electrostatic precipitator, the formalism of the rigid finite element method can be easily applied. Due to such an approach the equations of motion formulated contain a diagonal constant mass matrix and band stiffness matrix which is useful for numerical simulations. Indirect verifications of the method have been carried out. The software package developed on the basis of the model presented is designed for use by the producers of electrostatic precipitators. An intuitive interface can help at the initial stage of design. An influence of different parameters can be analysed without the necessity of formulating complex models using commercial software.

The paper is part of the project N R03 0035 04 financed by the National Centre for Research and Development

Manuscript received by Editorial Board, February 01, 2011;
final version, February 09, 2011.

REFERENCES

[1] Talaie M.R.: Mathematical modeling of wire-duct single-stage electrostatic precipitators, J. of Hazardous Materials, 2005, Vol.124, No.1-3, pp.44-52.
[2] Neimarlija N., Demirdžić I., Muzaferij S.: Finite volume method for calculation of electrostatic fields in electrostatic precipitators. J. of Electrostatics, 2009, Vol.67, No.1, pp.37-47.
[3] Long Z., Yao Q., Song Q., Li S.: A second-order accurate finite volume method for the computation of electrical conditions inside a wire-plate electrostatic precipitator on unstructured meshes, J. of Electrostatics, 2009, Vol.67, No.4, pp.597-604.
[4] Clack H.L.: Mass transfer within electrostatic precipitators: trace gas adsorption by sorbent-covered plate electrodes, J. of the Air & Waste Management Association, 2006, Vol. 56, No.6, pp. 759-766.
[5] Clack H.L.: Mercury capture within coal-fired power plant electrostatic precipitators: model evaluation, Environmental Science & Technology, 2009, Vol. 43, No.5, pp.1460-1466.

[6] Zienkiewicz O.C., Taylor R.L.: The finite element method Vol 2: Solid mechanics, 5th ed. Oxford: Butterworth-Heinemann, 2000.
[7] Kruszewski J., Gawroński W., Wittbrodt E., Najbar F., Grabowski S.: Metoda sztywnych elementów skończonych. Warsaw: Arkady, 1975.
[8] Wittbrodt E., Adamiec-Wójcik I., Wojciech S.: Dynamics of flexible multibody systems: rigid finite element method, Berlin: Springer, 2006.
[9] Nowak A.P., Adamiec-Wójcik I.: Vibration analysis of collecting electrodes of precipitators by means of the hybrid finite element method. Proc. Multibody Dynamics ECCOMAS Conference, 2009.
[10] Adamiec-Wójcik I., Nowak A.P., Wojciech S.: Dynamic analysis of electrostatic precipitators using finite strip method, Proc. 10th Conf. on Dynamical Systems – Theory and Applications DSTA, 2009, pp. 889-896.
[11] Adamiec-Wójcik I., Wojciech S.: Application of finite strip and rigid finite element methods to modelling of vibrations of collecting electrodes, Proc. of the 1st Joint International Conference on Multibody System Dynamics, 2010.
[12] Adamiec-Wójcik I., Wojciech S.: Numeryczne aspekty w modelowaniu drgań elektrofiltrów, 2010, Acta Mechanica et Automatica Vol. 4 No. 2, pp. 5-8.
[13] Adamiec-Wójcik I., Brzozowski K., Nowak A., Ryguła Cz., Wojciech S.: Analiza statyczna układów płyt zbiorczych elektrofiltrów Monografie Wydziału Inżynierii Mechanicznej i Robotyki AGH, 2010, no 42, pp.5-20.

Modelowanie układów płyt zbiorczych elektrofiltrów z wykorzystaniem metody sztywnych elementów skończonych

S t r e s z c z e n i e

W artykule przedstawiono model układu strzepującego elektrofiltru suchego. Układ strzepujący składa się z zestawu elektrod zbiorczych zawieszonych na belce górnej i ujętych w drąg strzepujący. Belki górna i dolna modelowane są przy pomocy metody sztywnych elementów skończonych podczas gdy do modelowania elektrod zbiorczych wykorzystywana jest hybrydowa metoda elementów skończonych. Metoda ta łączy metodę sztywnych elementów skończonych z klasyczną metodą elementów skończonych. W wyniku takiego podejścia otrzymuje się diagonalną macierz mas. W artykule przedstawiono wyniki symulacji numerycznych dotyczące drgań własnych płyt zbiorczych oraz wpływ liczby elementów, na które dzielono płyty, na drgania układu strzepującego.